Overhauser's spin-density wave in exact-exchange spin-density functional theory

S. Kurth[1,2,3] and F. G. Eich[4,5,3]
[1]*Nano-Bio Spectroscopy Group, Depto. de Física de Materiales, Universidad del País Vasco UPV/EHU, Centro Física de Materiales CSIC-UPV/EHU, Av. Tolosa 72, E-20018 San Sebastián, Spain*
[2]*IKERBASQUE, Basque Foundation for Science, E-48011 Bilbao, Spain*
[3]*European Theoretical Spectroscopy Facility (ETSF)*
[4]*Institut für Theoretische Physik, Freie Universität Berlin, Arnimallee 14, D-14195 Berlin, Germany*
[5]*Fritz Haber Institute of the Max Planck Society, Faradayweg 4-6, D-14195 Berlin, Germany*
(Received 19 June 2009; revised manuscript received 21 August 2009; published 23 September 2009)

The spin-density wave (SDW) state of the uniform electron gas is investigated in the exact-exchange approximation of noncollinear spin-density functional theory (DFT). Unlike in Hartree-Fock theory, where the uniform paramagnetic state of the electron gas is unstable against formation of the spin-density wave for all densities, in exact-exchange spin DFT this instability occurs only for densities lower than a critical value. It is also shown that, although in a suitable density range it is possible to find a noninteracting SDW ground-state Slater determinant with energy lower than the corresponding paramagnetic state, this Slater determinant is not a self-consistent solution of the optimized effective potential (OEP) integral equations of noncollinear spin DFT. A self-consistent solution of the OEP equations which gives an even lower energy can be found using an excited-state Slater determinant where only orbitals with single-particle energies in the lower of two bands are occupied while orbitals in the second band remain unoccupied even if their energies are below the Fermi energy.

DOI: 10.1103/PhysRevB.80.125120 PACS number(s): 71.10.Ca, 71.15.Mb, 75.30.Fv

I. INTRODUCTION

The *ab initio* description of noncollinear magnetic phenomena such as spin-density waves (SDWs) is typically based on an extension[1] of the original Kohn-Sham density functional theory (DFT).[2] As always in DFT, its success crucially relies on the accuracy of approximations for the exchange-correlation energy. An important step for the application of noncollinear DFT to real systems proved to be the construction of a noncollinear version of the local spin-density approximation (LSDA) by Kübler and co-workers.[3] An alternative density functional formalism for the description of SDWs and antiferromagnetism was proposed by Capelle and Oliveira.[4,5] In their work the system is not described in terms of its density and magnetization density as in usual spin DFT (SDFT) but instead in terms of the density and the so-called "staggered density" where the latter is a nonlocal quantity introduced to capture the nonlocal physics of SDWs and antiferromagnetic systems.

However, nonlocality may also be captured within the framework of usual SDFT if one abandons the local approximation to the exchange-correlation energy. Orbital functionals, i.e., functionals which explicitly depend on the single-particle orbitals rather than on the density (or densities), can be highly nonlocal. In DFT (or SDFT), the optimized effective potential (OEP) method[6–8] provides a framework to treat orbital functionals. This methodology has recently been generalized to the case of noncollinear magnetism.[9]

In the present work we use the noncollinear OEP method to study a very simple model system, the uniform electron gas. This model is of paramount importance in many-body physics.[10] Moreover, in his seminal work Overhauser[11,12] showed analytically that this simple model, if treated within the Hartree-Fock (HF) approximation, leads to an instability of the paramagnetic phase with respect to formation of a spin-density wave. In SDFT, the approximation analogous to HF is the exact-exchange (EXX) approximation which is the HF total-energy functional but evaluated with orbitals which come from both a *local* single-particle potential as well as a local magnetic field. Here we use the EXX approximation for a numerical investigation of Overhauser's SDW state in the framework of SDFT. This is complementary to another work[13] where Overhauser's SDW state is investigated numerically within HF and reduced density-matrix functional theory.

The paper is organized as follows: in Sec. II we briefly review the formalism of noncollinear SDFT and the corresponding OEP method. In Sec. III we minimize the EXX total energy for a given ansatz of the SDW state. In Sec. IV we investigate if the chosen ansatz is self-consistent in the framework of noncollinear SDFT before we provide our conclusions in Sec. V.

II. NONCOLLINEAR SPIN-DENSITY FUNCTIONAL THEORY

In noncollinear SDFT, a system of interacting electrons with ground state $|\Psi_0\rangle$ moving in an external electrostatic potential $v_0(\mathbf{r})$ (typically the electrostatic potential due to the nuclei) and magnetic field $\mathbf{B}_0(\mathbf{r})$ is described through its particle density

$$n(\mathbf{r}) = \langle \Psi_0 | \hat{\Psi}^\dagger(\mathbf{r}) \hat{\Psi}(\mathbf{r}) | \Psi_0 \rangle \tag{1}$$

and its magnetization density

$$\mathbf{m}(\mathbf{r}) = -\mu_B \langle \Psi_0 | \hat{\Psi}^\dagger(\mathbf{r}) \boldsymbol{\sigma} \hat{\Psi}(\mathbf{r}) | \Psi_0 \rangle. \tag{2}$$

Here, $\hat{\Psi}(\mathbf{r})$ is the field operator for Pauli spinors, μ_B is the Bohr magneton, and $\boldsymbol{\sigma}$ is the vector of Pauli matrices (atomic units are used throughout). For given external potentials, the total ground-state energy of such a system can be written as a functional of these two densities

$$E_{v_0,\mathbf{B}_0}[n,\mathbf{m}] = T_s[n,\mathbf{m}] + \int \mathrm{d}^3 r v_0(\mathbf{r}) n(\mathbf{r}) - \int \mathrm{d}^3 r \mathbf{B}_0(\mathbf{r}) \mathbf{m}(\mathbf{r}) + U[n] + E_{xc}[n,\mathbf{m}] + E_{ion}, \tag{3}$$

where $T_s[n,\mathbf{m}]$ is the noninteracting kinetic energy

$$U[n] = \frac{1}{2} \int \mathrm{d}^3 r \int \mathrm{d}^3 r' \frac{n(\mathbf{r}) n(\mathbf{r}')}{|\mathbf{r}-\mathbf{r}'|} \tag{4}$$

is the classical electrostatic energy of the electrons and E_{ion} is the classical electrostatic energy of the ions. $E_{xc}[n,\mathbf{m}]$ is the (unknown) exchange-correlation energy functional which has to be approximated in practice. Once an approximation for this functional is specified, the densities $n(\mathbf{r})$ and $\mathbf{m}(\mathbf{r})$ can be obtained as (ground-state) densities of a noninteracting system whose orbitals are given by self-consistent solution of the Kohn-Sham (KS) equation

$$\left(-\frac{\nabla^2}{2} + v_s(\mathbf{r}) + \mu_B \boldsymbol{\sigma} \mathbf{B}_s(\mathbf{r}) \right) \Phi_i(\mathbf{r}) = \varepsilon_i \Phi_i(\mathbf{r}), \tag{5}$$

where the $\Phi_i(\mathbf{r})$ are single-particle Pauli spinors. The effective potentials are given by

$$v_s(\mathbf{r}) = v_0(\mathbf{r}) + \int \mathrm{d}^3 r' \frac{n(\mathbf{r}')}{|\mathbf{r}-\mathbf{r}'|} + v_{xc}(\mathbf{r}) \tag{6}$$

and

$$\mathbf{B}_s(\mathbf{r}) = \mathbf{B}_0(\mathbf{r}) + \mathbf{B}_{xc}(\mathbf{r}) \tag{7}$$

with the exchange-correlation potentials

$$v_{xc}(\mathbf{r}) = \frac{\delta E_{xc}[n,\mathbf{m}]}{\delta n(\mathbf{r})} \tag{8}$$

and

$$\mathbf{B}_{xc}(\mathbf{r}) = -\frac{\delta E_{xc}[n,\mathbf{m}]}{\delta \mathbf{m}(\mathbf{r})}, \tag{9}$$

respectively.

In this work we will use the EXX energy functional as an approximation to the exchange-correlation energy which can be expressed in terms of the single-particle spinors Φ_i as

$$E_{\mathrm{EXX}}[\{\Phi_l\}] = -\frac{1}{2} \sum_{i,j}^{occ} \int \mathrm{d}^3 r \int \mathrm{d}^3 r' \frac{[\Phi_i^\dagger(\mathbf{r}) \cdot \Phi_j(\mathbf{r})][\Phi_j^\dagger(\mathbf{r}') \cdot \Phi_i(\mathbf{r}')]}{|\mathbf{r}-\mathbf{r}'|} \tag{10}$$

Since the EXX functional explicitly depends on the (spinor) orbitals but only implicitly on the densities, the calculation of the exchange-correlation potentials Eqs. (8) and (9) has to be performed by means of the OEP method.[6–8] A formulation of this technique for the case of noncollinear magnetism has recently been given in Ref. 9. The coupled OEP integral equations for the exchange-correlation potentials can be obtained by applying the chain rule of functional derivatives

$$\frac{\delta E_{xc}}{\delta v_s(\mathbf{r})} = \int \mathrm{d}^3 r' \left(v_{xc}(\mathbf{r}') \frac{\delta n(\mathbf{r}')}{\delta v_s(\mathbf{r})} - \mathbf{B}_{xc}(\mathbf{r}') \frac{\delta \mathbf{m}(\mathbf{r}')}{\delta v_s(\mathbf{r})} \right) = \sum_i^{occ} \int \mathrm{d}^3 r' \left(\frac{\delta E_{xc}}{\delta \Phi_i(\mathbf{r}')} \frac{\delta \Phi_i(\mathbf{r}')}{\delta v_s(\mathbf{r})} + H.c. \right), \tag{11}$$

$$\frac{\delta E_{xc}}{\delta \mathbf{B}_s(\mathbf{r})} = \int \mathrm{d}^3 r' \left(v_{xc}(\mathbf{r}') \frac{\delta n(\mathbf{r}')}{\delta \mathbf{B}_s(\mathbf{r})} - \mathbf{B}_{xc}(\mathbf{r}') \frac{\delta \mathbf{m}(\mathbf{r}')}{\delta \mathbf{B}_s(\mathbf{r})} \right) = \sum_i^{occ} \int \mathrm{d}^3 r' \left(\frac{\delta E_{xc}}{\delta \Phi_i(\mathbf{r}')} \frac{\delta \Phi_i(\mathbf{r}')}{\delta \mathbf{B}_s(\mathbf{r})} + H.c. \right) \tag{12}$$

The functional derivatives of the spinor orbitals and the densities with respect to the potentials can be computed from first-order perturbation theory and following the notation of Ref. 14 the OEP equations can be written in compact form as

$$\sum_i^{occ} [\Phi_i^\dagger(\mathbf{r}) \Psi_i(\mathbf{r}) + H.c.] = 0 \tag{13}$$

$$-\mu_B \sum_i^{occ} [\Phi_i^\dagger(\mathbf{r}) \boldsymbol{\sigma} \Psi_i(\mathbf{r}) + H.c.] = 0 \tag{14}$$

where we have defined the orbital shifts[7,15,16]

$$\Psi_i(\mathbf{r}) = \sum_{\substack{j \\ j \neq i}} \frac{D_{ij} \Phi_j(\mathbf{r})}{\varepsilon_i - \varepsilon_j} \tag{15}$$

with

$$D_{ij} = \int \mathrm{d}^3 r' \Phi_j^\dagger(\mathbf{r}') \times \left\{ [v_{xc}(\mathbf{r}') + \mu_B \boldsymbol{\sigma} \mathbf{B}_{xc}(\mathbf{r}')] \Phi_i(\mathbf{r}') - \frac{\delta E_{xc}}{\delta \Phi_i^\dagger(\mathbf{r}')} \right\}. \tag{16}$$

Equations (5)–(10), (13), and (14) constitute our formal framework to investigate the spin-density wave in the uniform electron gas in exact exchange.

III. UNIFORM ELECTRON GAS WITH SPIN-DENSITY WAVE: DIRECT MINIMIZATION OF ENERGY

We study a uniform electron gas, i.e., a system of electrons with spatially constant density moving in the electrostatic potential created by a neutralizing uniform density of positive background charge. In the following, rather than calculating the Kohn-Sham potentials self-consistently, we assume that the Kohn-Sham electrostatic potential $v_s(\mathbf{r})$ is a constant (which we set to zero) and that the Kohn-Sham magnetic field $\mathbf{B}_s(\mathbf{r})$ forms a spiral with amplitude B and wavevector $\mathbf{q}=q\mathbf{e}_z$ where $\mathbf{e}_z$ is a unit vector in z direction, i.e., $\mathbf{B}_s(\mathbf{r})=[B\cos(qz), B\sin(qz), 0]$. Moreover, we also assume that the Kohn-Sham magnetic field is entirely due to its exchange-correlation part, i.e., we study the system without external magnetic field. Of course, at some point we have to

verify that our assumptions are consistent within the SDFT framework. This question will be studied in Sec. IV.

With the effective potentials given above, the Kohn-Sham Eq. (5) can be solved analytically. A complete set of quantum numbers is given by a band index $b=1,2$ and a wavevector $\mathbf{k}$. The corresponding single-particle eigenstates and eigenenergies for the first band are given by

$$\Phi_{\mathbf{k}}^{(1)}(\mathbf{r}) = \frac{\exp(i\mathbf{kr})}{\sqrt{\mathcal{V}}} \begin{bmatrix} \cos\vartheta_{k_z} \\ \sin\vartheta_{k_z}\exp(iqz) \end{bmatrix}, \tag{17}$$

where $\mathcal{V}$ is the system volume (which tends to infinity) and

$$\varepsilon_{\mathbf{k}}^{(1)} = \frac{k_\parallel^2}{2} + \varepsilon_\kappa^{(1)} \tag{18}$$

where $k_\parallel = \sqrt{k_x^2 + k_y^2}$, $\kappa = k_z + \frac{q}{2}$, and

$$\varepsilon_\kappa^{(1)} = \frac{\kappa^2}{2} + \frac{q^2}{8} - \sqrt{\frac{q^2}{4}\kappa^2 + \mu_B^2 B^2}. \tag{19}$$

The angle ϑ_{k_z} is defined through the relation

$$\tan 2\vartheta_\kappa = -2\alpha \tag{20}$$

with

$$\alpha = \frac{\mu_B B}{q\kappa}. \tag{21}$$

For the second band the eigenstates and eigenenergies are

$$\Phi_{\mathbf{k}}^{(2)}(\mathbf{r}) = \frac{\exp(i\mathbf{kr})}{\sqrt{\mathcal{V}}} \begin{bmatrix} -\sin\vartheta_{k_z} \\ \cos\vartheta_{k_z}\exp(iqz) \end{bmatrix} \tag{22}$$

and

$$\varepsilon_{\mathbf{k}}^{(2)} = \frac{k_\parallel^2}{2} + \varepsilon_\kappa^{(2)} \tag{23}$$

with

$$\varepsilon_\kappa^{(2)} = \frac{\kappa^2}{2} + \frac{q^2}{8} + \sqrt{\frac{q^2}{4}\kappa^2 + \mu_B^2 B^2}. \tag{24}$$

In order for the definition of $\Phi_{\mathbf{k}}^{(1)}(\mathbf{r})$ and $\Phi_{\mathbf{k}}^{(2)}(\mathbf{r})$ to be unique, the angle ϑ_κ has to be restricted to an interval of length $\pi/2$. Assuming that $B \geq 0$ and $q > 0$, we find from Eq. (20) that $-\pi/2 < \vartheta_\kappa \leq 0$. Using a trigonometric identity we can transform Eq. (20) to

$$\tan\vartheta_\kappa = \frac{1}{2\alpha}(1 - \sqrt{1+4\alpha^2}) \tag{25}$$

From Eq. (20) we see that for finite B and $\kappa=0$ the angle $\vartheta_{\kappa=0} = -\frac{\pi}{4}$. In order for ϑ_κ to be a continuous function of κ with values in the correct range we invert Eq. (25) as

$$\vartheta_\kappa = \begin{cases} \arctan\left[\frac{1}{2\alpha}(1-\sqrt{1+4\alpha^2})\right] & \text{for } \kappa \geq 0 \\ -\frac{\pi}{2} + \arctan\left[\frac{1}{2\alpha}(1-\sqrt{1+4\alpha^2})\right] & \text{for } \kappa < 0 \end{cases}. \tag{26}$$

With the single-particle states fully defined we can write down the uniform electronic (ground-state) density as

$$n = \sum_b n^{(b)} = \sum_b \int \frac{\mathrm{d}^3k}{(2\pi)^3}\theta(\varepsilon_F - \varepsilon_{\mathbf{k}}^{(b)}) = \frac{1}{4\pi^2}\sum_b \int \mathrm{d}\kappa\,\theta(\varepsilon_F - \varepsilon_\kappa^{(b)})(\varepsilon_F - \varepsilon_\kappa^{(b)}), \tag{27}$$

where $n^{(b)}$ is the density contribution of band b, $\theta(x)$ is the Heaviside step function and the trivial integrals have been carried out in the last step. Using Eqs. (18) and (23), the integration limits can be determined analytically and the remaining integral can easily be solved in closed form but we refrain from giving the explicit expression here.

Similarly, we can compute the magnetization density. We obtain for the x and y components

$$m_x(\mathbf{r}) = m_0\cos(qz) \tag{28}$$

and

$$m_y(\mathbf{r}) = m_0\sin(qz), \tag{29}$$

where the amplitude of the spin-density wave is

$$m_0 = -\frac{\mu_B}{2\pi^2}\sum_b \mathrm{sign}(b) \times \int \mathrm{d}\kappa\,\theta(\varepsilon_F - \varepsilon_\kappa^{(b)})(\varepsilon_F - \varepsilon_\kappa^{(b)})\sin\vartheta_\kappa\cos\vartheta_\kappa \tag{30}$$

and we have defined

$$\mathrm{sign}(b) = \begin{cases} +1 & \text{for } b=1 \\ -1 & \text{for } b=2 \end{cases}. \tag{31}$$

Using the symmetry relation $\theta_{-\kappa} = -\frac{\pi}{2} - \theta_\kappa$ [see Eq. (26)], the z component of the magnetization density can be shown to vanish identically

$$m_z(\mathbf{r}) = 0. \tag{32}$$

We point out that the vector of the magnetization density here is parallel to the Kohn-Sham magnetic field. This certainly is a consequence of the simplicity of the system under study here. For more complicated systems it was shown in Ref. 9 that these quantities need not be parallel in noncollinear SDFT in EXX. This is an important difference to the noncollinear LSDA formulation of Ref. 3 where the magnetization density and the exchange-correlation magnetic field are locally parallel by construction.

We now turn to the evaluation of the energy of Eq. (3) and note that for an electrically neutral system with uniform ionic and electronic densities the sum of the ionic energy E_{ion}, the electronic interaction with the ionic potential $\int \mathrm{d}^3 r v_0(\mathbf{r}) n(\mathbf{r})$

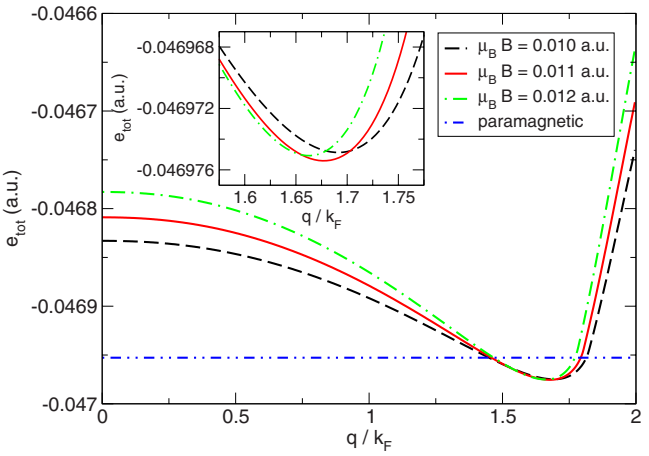

FIG. 1. (Color online) Total energy per particle in EXX for the electron gas at $r_s=5.4$ with spin-density wave as function of q/k_F and different values of the amplitude B of the Kohn-Sham magnetic field. The straight line corresponds to the total energy per particle of the paramagnetic state at this density. The inset shows a magnification close to the minimum.

and the Hartree energy $U[n]$ exactly cancels out. We study the system at vanishing external magnetic field, $\mathbf{B}_0(\mathbf{r})\equiv 0$, and use the exact-exchange energy of Eq. (10) as an approximation to the exchange-correlation energy functional. It is expected[10,17] that inclusion of correlation leads to SDW states higher in energy than the paramagnetic states.

In our case the total energy per unit volume only consists of a kinetic and an exchange contribution, i.e.,

$$\tilde{e}_{tot}=\tilde{t}_s+\tilde{e}_{\mathrm{EXX}}. \tag{33}$$

The kinetic energy per unit volume has contributions from the two bands

$$\tilde{t}_s=\frac{T_s}{\mathcal{V}}=\sum_b \tilde{t}_s^{(b)}, \tag{34}$$

where the contribution of the first band is given by

$$\tilde{t}_s^{(1)}=\frac{1}{8\pi^2}\int \mathrm{d}\kappa\,\theta(\varepsilon_F-\varepsilon_\kappa^{(1)})(\varepsilon_F-\varepsilon_\kappa^{(1)}) \times\left(\varepsilon_F-\varepsilon_\kappa^{(1)}+\kappa^2+\frac{q^2}{4}+2q\kappa\sin^2\vartheta_\kappa\right) \tag{35}$$

while the contribution of the second band is

$$\tilde{t}_s^{(2)}=\frac{1}{8\pi^2}\int \mathrm{d}\kappa\,\theta(\varepsilon_F-\varepsilon_\kappa^{(2)})(\varepsilon_F-\varepsilon_\kappa^{(2)}) \times\left(\varepsilon_F-\varepsilon_\kappa^{(2)}+\kappa^2+\frac{q^2}{4}+2q\kappa\cos^2\vartheta_\kappa\right). \tag{36}$$

Inserting the orbitals (17) and (22) into Eq. (10), the exchange energy per unit volume, $\tilde{e}_{\mathrm{EXX}}$, can also be expressed as sum of two terms

$$\tilde{e}_{\mathrm{EXX}}=\tilde{e}_{\mathrm{EXX}}^{(1)}+\tilde{e}_{\mathrm{EXX}}^{(2)}. \tag{37}$$

The first term which describes intraband exchange is, after carrying out the angular integrals, given by

$$\tilde{e}_{\mathrm{EXX}}^{(1)}=-\frac{1}{32\pi^3}\sum_b\int \mathrm{d}\kappa\,\theta(\varepsilon_F-\varepsilon_\kappa^{(b)})\int \mathrm{d}\kappa'\,\theta(\varepsilon_F-\varepsilon_{\kappa'}^{(b)}) \times\cos^2(\vartheta_\kappa-\vartheta_{\kappa'})I[y^{(b)}(\kappa),y^{(b)}(\kappa'),(\kappa-\kappa')^2] \tag{38}$$

while the second term, describing interband exchange, reads

$$\tilde{e}_{\mathrm{EXX}}^{(2)}=-\frac{1}{16\pi^3}\int \mathrm{d}\kappa\,\theta(\varepsilon_F-\varepsilon_\kappa^{(1)})\int \mathrm{d}\kappa'\,\theta(\varepsilon_F-\varepsilon_{\kappa'}^{(2)}) \times\sin^2(\vartheta_\kappa-\vartheta_{\kappa'})I[y^{(1)}(\kappa),y^{(2)}(\kappa'),(\kappa-\kappa')^2]. \tag{39}$$

where we have defined

$$y^{(b)}(\kappa)=2(\varepsilon_F-\varepsilon_\kappa^{(b)}). \tag{40}$$

In Eqs. (38) and (39) we also have used the integral

$$I(y_1,y_2,a)=\int_0^{y_1}\mathrm{d}y\int_0^{y_2}\mathrm{d}y'\,\frac{1}{\sqrt{(y-y')^2+2(y+y')a+a^2}} \tag{41}$$

which can be solved in closed form by transforming to new integration variables $z=y-y'$ and $z'=(y+y')/2$ and changing the integration limits accordingly. Therefore the calculation of the total energy only requires the numerical calculation of a two-dimensional integral.

We have calculated the total energy per particle

$$e_{tot}=\frac{\tilde{e}_{tot}}{n} \tag{42}$$

in the following way: we start by numerically calculating the Fermi energy for a given value n of the density or, equivalently, the Wigner-Seitz radius

$$r_s=\left(\frac{3}{4\pi n}\right)^{1/3} \tag{43}$$

and given values of the parameters B and q from Eq. (27). The Fermi energy thus becomes a function of these three parameters

$$\varepsilon_F=\varepsilon_F(r_s,q,B), \tag{44}$$

which is then used to evaluate the total energy per particle for these parameter values. We then have, for fixed r_s, minimized e_{tot} as a function of the parameters q and B numerically.

In Fig. 1 we show the total energy per electron at $r_s=5.4$ for a few values of B as function of q/k_F where

$$k_F=\left(\frac{9\pi}{4}\right)^{1/3}\frac{1}{r_s} \tag{45}$$

is the Fermi wave number of the uniform electron gas in the paramagnetic state. The value $r_s=5.4$ was chosen because then (i) the SDW phase is lower in energy than both the paramagnetic and ferromagnetic phases and (ii) the amplitude of the SDW (or the KS magnetic field) is relatively high such that the resulting energy differences can easily be resolved numerically. We clearly see that for the given values

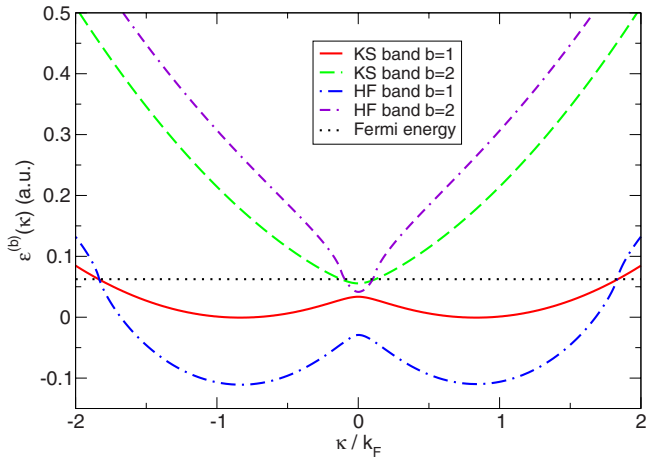

FIG. 2. (Color online) Single-particle KS and HF bands at $k_{\|}=0$ for the optimized parameter values ($\mu_B B=0.011$ a.u. and $q/k_F=1.68$ at $r_s=5.4$) minimizing the EXX total energy per particle in Fig. 1. The straight line indicates the Fermi energy and shows that close to $\kappa/k_F=0$ states of the second KS band [dashed (green) line] are occupied in the ground state. The KS orbitals have been used to compute the HF Hamiltonian and the resulting HF bands have been shifted rigidly such that the lower HF and KS bands equal ε_F at the same value of $|\kappa/k_F|$. The relative position of the second HF band [dash-dash-dotted (purple) line] indicates that also in HF states in both bands will be occupied.

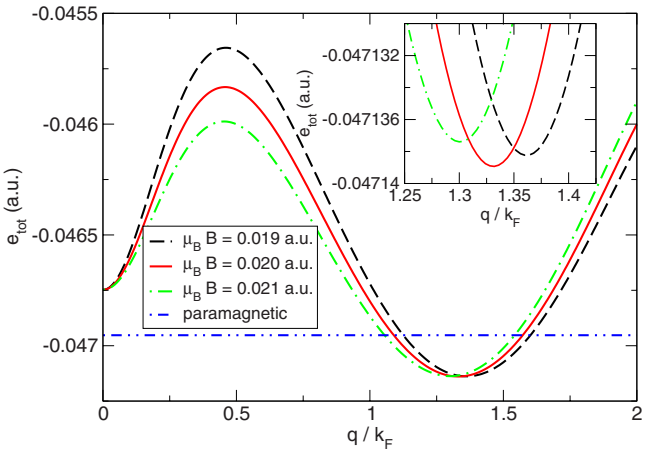

FIG. 3. (Color online) Same as Fig. 1 except that now only states in the lower band are allowed to be occupied. The total energy per particle at the minimum is lower than when states in both bands are allowed to be occupied.

of B for wave numbers between $q/k_F\approx 1.5$ and $q/k_F\approx 1.75$ the energy of the SDW state is lower than the energy of the paramagnetic state. The lowest energy for this value of r_s is achieved for the parameters $\mu_B B=0.011$ a.u. and $q/k_F=1.68$.

In Fig. 2 we show the KS single-particle dispersions of Eqs. (18) and (23) as well as the HF single-particle dispersions. To obtain the latter ones we first calculate the HF self-energy (which is a 2×2 matrix in spin space) as

$$\Sigma^{\mathrm{HF}}(\mathbf{r},\mathbf{r}') = -\sum_b \sum_{\mathbf{k}} \theta(\varepsilon_F - \varepsilon_{\mathbf{k}}^{(b)}) \frac{\Phi_{\mathbf{k}}^{(b)}(\mathbf{r}) \otimes \Phi_{\mathbf{k}}^{(b)\dagger}(\mathbf{r}')}{|\mathbf{r}-\mathbf{r}'|} \tag{46}$$

and then diagonalize the resulting HF Hamiltonian

$$\hat{h}^{\mathrm{HF}} = -\frac{\nabla^2}{2} + \int \mathrm{d}^3 r' \Sigma^{\mathrm{HF}}(\mathbf{r},\mathbf{r}') \ldots , \tag{47}$$

where the second term is a to be read as an integral operator. We would like to emphasize that we use the KS orbitals and orbital energies to evaluate the HF self energy, i.e., we do *not* perform a self-consistent HF calculation here.

In Fig. 2 we show the KS and HF dispersions only for the κ coordinate, i.e., we set $k_{\|}=0$. As expected, close to $\kappa/k_F=0$ a direct gap opens up in the KS single-particle dispersions due to the presence of the spin-density wave. The position of the Fermi energy is such that not only states of the lower ($b=1$) band but also states of the second ($b=2$) KS band are occupied in the ground state.

The HF bands in Fig. 2 have been rigidly shifted by a constant such that the lower HF band ($b=1$) and the lower KS band equal the Fermi energy for the *same* value of κ/k_F. It is evident that, as expected, the HF single-particle direct band gap at $\kappa/k_F=0$ is much larger than the corresponding KS gap. Moreover, the position of the second HF band indicates that also in the HF case there will be occupied states in the second band. While here we have calculated the HF bands using the DFT orbitals and orbital energies, we have confirmed[13] that the above statement is true also for a HF energy minimization and the resulting HF bands are very close to the ones presented here.

The occupation of states in both single-particle bands is sometimes excluded in works on the SDW in the Hartree-Fock approximation[10,12] and also in a numerical investigation[13] we have found that for the global energy minimum in Hartree Fock only the lowest single-particle band is occupied. This has motivated us to do the minimization of the total energy in EXX also under the additional constraint that only states of the lowest subband are occupied.

Similar to Fig. 1, in Fig. 3 we show the total energy per electron at $r_s=5.4$ for a few values of B as function of q/k_F. Of course, the constrained minimization leads, for a given value of r_s, to different optimized parameter values. Surprisingly, however, we found that the minimization constraining the occupation to the lower subband *leads to lower total energies* than the ones obtained with a two-band minimization. Moreover, this lower total energy is achieved with a Slater determinant *which has empty states below the Fermi level.*

This can be seen in Fig. 4 where we show the KS and HF energy bands at $r_s=5.4$ for this "one-band" minimization for the optimized parameter values of $\mu_B B=0.020$ a.u. and $q/k_F=1.33$. We see that there are states in the second KS band below the Fermi energy which, due to the constraint in the minimization, remain unoccupied. We also note that for the one-band case the amplitude of the minimizing Kohn-Sham magnetic field, and therefore also the "gap" between the two KS bands at $\kappa/k_F=0$, is almost twice as large as in the two-band case. Compared to Fig. 2, the intersection of the Fermi energy with the bands $\varepsilon^{(b)}(\kappa)$ is shifted to a lower value of $|\kappa|$.

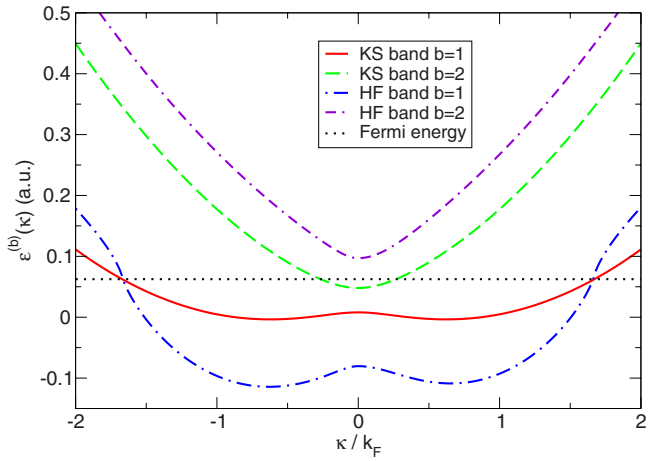

FIG. 4. (Color online) Same as Fig. 2 except that the optimized parameters are used which result from a minimization with occupied states in the lower KS band only. For r_s=5.4 these values are $\mu_B B$=0.020 a.u. and q/k_F=1.33. Again, the straight line indicates the Fermi energy. Note that the states of the second KS band [dashed (green) line] remain unoccupied in this calculation, even if their single-particle energies are below the Fermi level, i.e., the resulting Slater determinant is not a ground state of the Kohn-Sham problem. On the other hand, the post-hoc evaluation of the HF bands (for details see caption of Fig. 2 and the main text) indicates that the second HF band [dash-dash-dotted (purple) line] will remain unoccupied and the resulting HF wave function will be a ground-state Slater determinant.

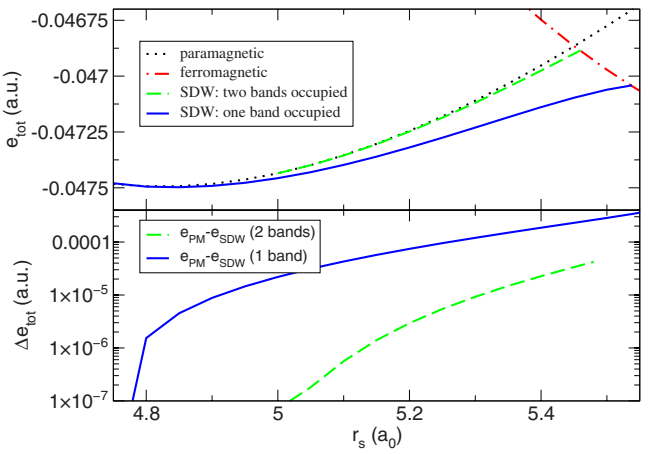

FIG. 5. (Color online) Upper panel: total energy per particle in EXX for different phases of the uniform electron gas as function of Wigner-Seitz radius r_s. In the SDW phase, in one case the occupation of single-particle states in both bands is allowed while in the other case the occupied states are restricted to the lower band. Lower panel: energy difference between the total energies per particle of the paramagnetic phase and the SDW phase for SDWs with occupied states in one and two bands. For the two-band case, the SDW phase is lower in energy than both the paramagnetic and the ferromagnetic phase for $5.0 \lesssim r_s \lesssim 5.46$. For the one-band case the range of stability of the SDW phase is $4.78 \lesssim r_s \lesssim 5.54$.

The HF bands again have rigidly been shifted such that the lower HF and KS bands intersect the Fermi energy at the same κ. Again, the direct HF gap at $\kappa/k_F=0$ is significantly larger than the KS gap. In contrast to the two-band case, the second HF band now is energetically higher than the Fermi energy and the corresponding HF state would, unlike the EXX state, have no unoccupied single-particle states below ε_F. Again here we have done only a post-hoc evaluation of the HF bands but we have checked that the statement remains valid for a self-consistent HF calculation as well.[13]

We have optimized the EXX total energy per particle for a range of r_s values once for single-particle occupations in both energy bands and once for occupations restricted to the lower band. In Fig. 5 we show the resulting phase diagram in the relevant density range. When allowing occupations in both bands, the SDW state (which is then a ground-state Slater determinant) is lower in energy than both the paramagnetic and the ferromagnetic phase for r_s in the range $5.0 \lesssim r_s \lesssim 5.46$. In this case the energies are very close to the energies of the paramagnetic phase (energy differences of less than 4×10^{-5} a.u., see lower panel of Fig. 5) and therefore the transition to the ferromagnetic phase occurs at an value of r_s only slightly higher than the r_s value where paramagnetic and ferromagnetic phases are degenerate.

On the other hand, restricting the single-particle occupation to the lowest band, the SDW state is more stable than paramagnetic and ferromagnetic state for $4.78 \lesssim r_s \lesssim 5.54$. In this case the energy differences between the paramagnetic and the SDW phase range to almost 4×10^{-4} a.u. (lower panel of Fig. 5), almost an order of magnitude larger than in the two-band case. However, for all r_s values in the stability range of the SDW phase, the minimizing Slater determinant in the one-band case is *not* a ground state of the Kohn-Sham problem.

Both the one- and two-band cases in EXX have in common that they predict the SDW phase to be lower in energy than the paramagnetic phase only for a restricted range of r_s values. This is different from the Hartree-Fock case[10,12] where the SDW phase is more stable than the paramagnetic phase for *all* values of r_s. This is not completely surprising since due to the additional constraint of local Kohn-Sham potentials v_s and $\mathbf{B}_s$ in the EXX minimization, the resulting energies have to be higher than the Hartree-Fock total energies. Since for small values of r_s the SDW total energies in HF are extremely close to the total energies of the paramagnetic phase,[13] the higher EXX total energies can easily lead to a more stable paramagnetic phase.

In Fig. 6 we show the SDW parameters q (upper panel) and B (middle panel) for which the EXX total energy per particle is minimized in the one- and two-band cases for those r_s values for which the SDW phase is more stable than both paramagnetic and ferromagnetic phases. For the one-band case, the wave number q of the spin-density wave covers almost the whole range between k_F and $2k_F$ while for the two-band case this range is much narrower. The amplitudes B and m_0 of the Kohn-Sham magnetic field (middle panel) and the magnetization density (lower panel) of the SDW are significantly smaller in the two-band case as for the case with occupied single-particle states in one band only. It is sometimes assumed[10] that the wave number of the SDW is close to $2k_F$. Our results show that this need not be the case, as in the one-band case q approaches k_F for densities at the lower

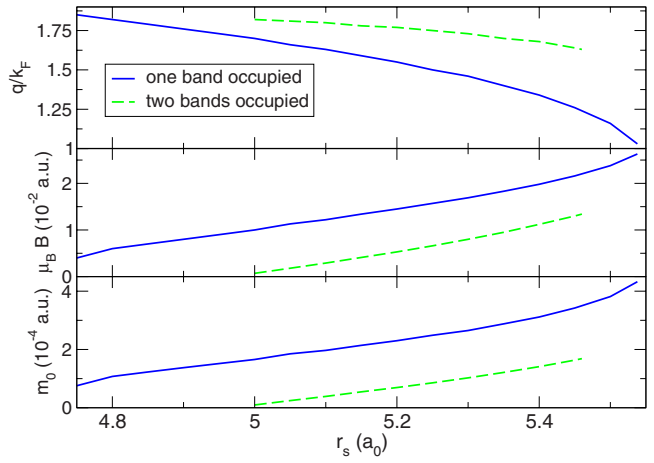

FIG. 6. (Color online) Optimized values for the parameters q (upper panel) and B (middle panel) for which the EXX total energy per particle of the SDW phase is minimized. The results are shown over the range of r_s values for which the SDW phase is lower in energy than both the paramagnetic and the ferromagnetic phases for the cases when both bands or only one band are occupied. Lower panel: amplitude of the SDW [Eq. (30)] for the one- and two-band case.

end of the stability range of the SDW phase. However, neither in EXX nor in HF (Ref. 13) have we ever found a stable SDW state with wave number lower than k_F.

IV. SELF-CONSISTENCY

In the previous Section we have used an ansatz for the Kohn-Sham orbitals in the SDW phase which depends on two parameters and then minimized the EXX total energy per particle with respect to these parameters. We have done this minimization once allowing single-particle states in both bands to be occupied and once for occupations only in the lower band. This is different from the usual way of applying DFT where one calculates the exchange-correlation potentials and solves the Kohn-Sham equation self-consistently. In our case, the calculation of the EXX potentials requires solution of the OEP Eqs. (13) and (14). In the present Section we still use our ansatz for the Kohn-Sham orbitals and investigate if it is consistent with the OEP equations.

We start by calculating the orbital shifts of Eq. (15) in the EXX approximation. Inserting our ansatz after some straightforward algebra we obtain for the orbital shift of the first band

$$\Psi_{\mathbf{k}}^{(1)}(\mathbf{r}) = \frac{G(\mathbf{k})}{\varepsilon_\kappa^{(1)} - \varepsilon_\kappa^{(2)}} \Phi_{\mathbf{k}}^{(2)}(\mathbf{r}) \tag{48}$$

while the shift for the second band reads

$$\Psi_{\mathbf{k}}^{(2)}(\mathbf{r}) = -\frac{G(\mathbf{k})}{\varepsilon_\kappa^{(1)} - \varepsilon_\kappa^{(2)}} \Phi_{\mathbf{k}}^{(1)}(\mathbf{r}), \tag{49}$$

where we have defined

$$G(\mathbf{k}) = -q\kappa \sin\vartheta_\kappa \cos\vartheta_\kappa + F(\mathbf{k}) \tag{50}$$

as well as

$$F(\mathbf{k}) = \sum_b \mathrm{sign}(b) \int \frac{\mathrm{d}^3 k_1}{(2\pi)^3} \theta(\varepsilon_F - \varepsilon_{\mathbf{k}_1}^{(b)}) \times \frac{4\pi}{|\mathbf{k} - \mathbf{k}_1|^2} \sin(\vartheta_{\kappa_1} - \vartheta_\kappa)\cos(\vartheta_{\kappa_1} - \vartheta_\kappa). \tag{51}$$

Inserting the orbital shifts [Eqs. (48) and (49)] as well as the orbitals [Eqs. (17) and (22)] it is straightforward to see that the first OEP Eq. (13) is satisfied by our ansatz, i.e.,

$$\sum_b \sum_{\mathbf{k}} \theta(\varepsilon_F - \varepsilon_{\mathbf{k}}^{(b)}) [\Phi_{\mathbf{k}}^{(b)\dagger}(\mathbf{r}) \Psi_{\mathbf{k}}^{(b)}(\mathbf{r}) + \text{c.c.}] = 0. \tag{52}$$

This can easily be understood from the physical content of the OEP equations: if we start from the KS Hamiltonian as noninteracting reference and perform a perturbation expansion of the interacting density in the perturbation $\hat{W}_{Clb} - \hat{V}_{xc} - \mu_B \boldsymbol{\sigma} \hat{\mathbf{B}}_{xc}$, where $\hat{W}_{Clb}$ is the operator of the electron-electron interaction and $\hat{V}_{xc} + \mu_B \boldsymbol{\sigma} \hat{\mathbf{B}}_{xc}$ is the operator of the KS exchange-correlation potentials, then the OEP equation in EXX simply says that the density remains unchanged to first order. In our case we keep the density fixed and therefore the OEP Eq. (13) holds.

A similar argument can be used for the z component of the OEP Eq. (14) which says that the z component $m(\mathbf{r})$ of the magnetization density remains unchanged under the same perturbation to first order. This equation reads explicitly

$$\sum_b \sum_{\mathbf{k}} \theta(\varepsilon_F - \varepsilon_{\mathbf{k}}^{(b)}) [\Phi_{\mathbf{k}}^{(b)\dagger}(\mathbf{r}) \sigma_z \Psi_{\mathbf{k}}^{(b)}(\mathbf{r}) + \text{c.c.}] = -2 \sum_b \mathrm{sign}(b) \int \frac{\mathrm{d}^3 k}{(2\pi)^3} \theta(\varepsilon_F - \varepsilon_{\mathbf{k}}^{(b)}) \frac{\sin\vartheta_\kappa \cos\vartheta_\kappa G(\mathbf{k})}{\varepsilon_\kappa^{(1)} - \varepsilon_\kappa^{(2)}} = 0, \tag{53}$$

where the last equality can most easily be seen by noting that the integrand is an odd function under the transformation $\kappa \to -\kappa$ and all the integrals are over a symmetric range around $\kappa = 0$.

For the x and y component of Eq. (14) we obtain

$$\sum_b \sum_{\mathbf{k}} \theta(\varepsilon_F - \varepsilon_{\mathbf{k}}^{(b)}) [\Phi_{\mathbf{k}}^{(b)\dagger}(\mathbf{r}) \sigma_x \Psi_{\mathbf{k}}^{(b)}(\mathbf{r}) + \text{c.c.}] = J(\varepsilon_F, q, B)\cos(qz) = 0 \tag{54}$$

and

$$\sum_b \sum_{\mathbf{k}} \theta(\varepsilon_F - \varepsilon_{\mathbf{k}}^{(b)}) [\Phi_{\mathbf{k}}^{(b)\dagger}(\mathbf{r}) \sigma_x \Psi_{\mathbf{k}}^{(b)}(\mathbf{r}) + \text{c.c.}] = J(\varepsilon_F, q, B)\sin(qz) = 0, \tag{55}$$

where

$$J(\varepsilon_F, q, B) = 2 \sum_b \mathrm{sign}(b) \int \frac{\mathrm{d}^3 k}{(2\pi)^3} \theta(\varepsilon_F - \varepsilon_{\mathbf{k}}^{(b)}) \times \frac{(\cos^2\vartheta_\kappa - \sin^2\vartheta_\kappa) G(\mathbf{k})}{\varepsilon_\kappa^{(1)} - \varepsilon_\kappa^{(2)}}. \tag{56}$$

Since Eqs. (54) and (55) have to be satisfied for all values of z, we obtain only the condition

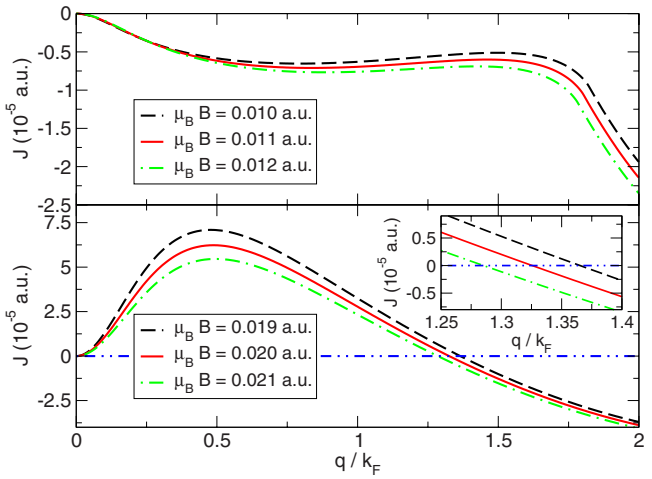

FIG. 7. (Color online) Upper panel: J of Eq. (56) for r_s=5.4 as function of q/k_F and different values of B for the case with occupations in two bands. The parameter values are the same as in Fig. 1 for which a minimum in the total energy per particle was found. Since J never crosses zero, in this case the minimum of the total energy is not consistent with the solution of the OEP equation. Lower panel: same as above but now for occupied single-particle states only in the lower band. The parameter values are the same as in Fig. 3. In contrast to the two-band case, now J not only crosses zero but also does so at those values of q/k_F for which a local minimum was found in Fig. 3 (see inset for magnification around the intersections with the zero axis). Therefore, the OEP equation in this case is consistent with the minimization of the total energy per particle.

$$J(\varepsilon_F, q, B) = 0, \tag{57}$$

i.e., the two OEP equations are not independent.

In Fig. 7 we show J of Eq. (56) for r_s=5.4 as function of q/k_F for different values of B both for the case of occupations in both bands (upper panel) as well as for occupations restricted to the lower band (lower panel). Note that for the latter case the sum over bands b both in Eq. (56) as well as in Eq. (51) only extends over the lower band, b=1.

In the upper panel of Fig. 7 we choose the same values for the parameter B as used in Fig. 1 which all had local minima for some value of $q < 2k_F$. For these values of B, however, Eq. (57) is not satisfied for any value of q in that range. We therefore have to conclude that in the two-band case the energy minimization is *not consistent with the OEP equations*.

In the lower panel of Fig. 7 where only single-particle states of the lower band are occupied we choose the parameters as in Fig. 3. In this case, J not only crosses zero but also does so exactly for those values of q/k_F for which we found local minima in the total energy per particle in Fig. 7 (see inset for a magnification of the region where J crosses zero). We therefore conclude that in the one-band case the minimization of the total energy is consistent with the OEP equation, i.e., our ansatz is self-consistent in this case. Again we emphasize that the resulting Slater determinant is *not* the ground state of the KS system.

It has been shown[18] that in unrestricted HF theory all the single-particle levels are fully occupied up to the Fermi energy. To the best of our knowledge, a similar statement has not been proven for DFT (even in EXX approximation) and our results indicate that it might not be true in EXX. On the other hand, the proof of Ref. 18 holds for the true, unrestricted HF ground state while in our case we have restricted the symmetry of our problem to the SDW symmetry. It is quite conceivable that the fact that we find an excited-state Slater determinant as energy-minimizing wave-function hints toward an instability of the SDW phase against further reduction in the symmetry.

V. SUMMARY AND CONCLUSIONS

We have investigated the SDW state of the uniform electron gas within the EXX approximation of noncollinear SDFT. While in the Hartree-Fock approximation the SDW state is energetically more stable than the paramagnetic state for all values of r_s, in EXX this is only true for values of r_s larger than a critical value. Using an explicit ansatz for the spinor orbitals in the SDW state, we have performed the energy minimization of the EXX total energy in two ways: (i) in the first case we used as noninteracting reference wave function a *ground-state* Slater determinant with occupied single-particle orbitals belonging to both single-particle energy bands, as long as their energy is below the Fermi energy. Then the SDW phase is more stable than both paramagnetic and ferromagnetic phases for $5.0 \lesssim r_s \lesssim 5.46$. (ii) In the second case we required all the occupied single-particle orbitals in the Slater determinant to belong to the lower band. The minimizing Slater determinant in this case turns out to be an excited state since orbitals with orbital energies below the Fermi energy belonging to the second band remain unoccupied. Nevertheless, for a given r_s the total energies of the minimizing SDW states are significantly lower than in case (i). The range of stability of the SDW phase with respect to both paramagnetic and ferromagnetic phases is extended to $4.78 \lesssim r_s \lesssim 5.54$.

We then have investigated if the self-consistency conditions provided by the OEP equations for noncollinear SDFT are satisfied with our ansatz for the single-particle orbitals. We have found that for case (i) the parameter values minimizing the EXX total energy are not consistent with a solution of the OEP equations. In case (ii), on the other hand, for the same parameter values for which the EXX total energy is minimized also the OEP equations are satisfied. In this case, the solution we found is therefore self-consistent.

ACKNOWLEDGMENTS

We would like to acknowledge useful discussions with Ilya Tokatly, Giovanni Vignale, and Nicole Helbig. We acknowledge funding by the "Grupos Consolidados UPV/EHU del Gobierno Vasco" (Grant No. IT-319-07).

[1] U. von Barth and L. Hedin, J. Phys. C **5**, 1629 (1972).
[2] W. Kohn and L. J. Sham, Phys. Rev. **140**, A1133 (1965).
[3] J. Kübler, K.-H. Höck, J. Sticht, and A. R. Williams, J. Phys. F **18**, 469 (1988).
[4] K. Capelle and L. N. Oliveira, Europhys. Lett. **49**, 376 (2000).
[5] K. Capelle and L. N. Oliveira, Phys. Rev. B **61**, 15228 (2000).
[6] J. D. Talman and W. F. Shadwick, Phys. Rev. A **14**, 36 (1976).
[7] T. Grabo, T. Kreibich, S. Kurth, and E. K. U. Gross, in *Strong Coulomb Correlations in Electronic Structure Calculations: Beyond Local Density Approximations*, edited by V. Anisimov (Gordon and Breach, Amsterdam, 2000), p. 203.
[8] S. Kümmel and L. Kronik, Rev. Mod. Phys. **80**, 3 (2008).
[9] S. Sharma, J. K. Dewhurst, C. Ambrosch-Draxl, S. Kurth, N. Helbig, S. Pittalis, S. Shallcross, L. Nordström, and E. K. U. Gross, Phys. Rev. Lett. **98**, 196405 (2007).
[10] G. Giuliani and G. Vignale, *Quantum Theory of the Electron Liquid* (Cambridge University Press, Cambridge, 2005).
[11] A. W. Overhauser, Phys. Rev. Lett. **4**, 462 (1960).
[12] A. W. Overhauser, Phys. Rev. **128**, 1437 (1962).
[13] F. G. Eich, S. Kurth, C. R. Proetto, S. Sharma, and E. K. U. Gross (unpublished).
[14] S. Kurth and S. Pittalis, in *Computational Nanoscience: Do It Yourself!*, NIC Series, edited by J. Grotendorst, S. Blügel, and D. Marx (John von Neumann Institute for Computing, Jülich, 2006), Vol. 31, p. 299.
[15] S. Kümmel and J. P. Perdew, Phys. Rev. Lett. **90**, 043004 (2003).
[16] S. Kümmel and J. P. Perdew, Phys. Rev. B **68**, 035103 (2003).
[17] G. F. Giuliani and G. Vignale, Phys. Rev. B **78**, 075110 (2008).
[18] V. Bach, E. H. Lieb, M. Loss, and J. P. Solovej, Phys. Rev. Lett. **72**, 2981 (1994).